

# Modulating the fundamental inductive-capacitive resonance in asymmetric double-split ring terahertz metamaterials

Yuanmu Yang,<sup>1</sup> Ran Huang,<sup>2</sup> Longqing Cong,<sup>1</sup> Zhihua Zhu,<sup>1</sup> Jianqiang Gu,<sup>1</sup> Zhen Tian,<sup>1</sup> Ranjan Singh,<sup>2,3</sup> Shuang Zhang,<sup>4</sup> Jiaguang Han,<sup>1,a)</sup> and Weili Zhang<sup>1,2,b)</sup>

<sup>1</sup>Center for Terahertz Waves and College of Precision Instrument and Optoelectronics Engineering, Tianjin University, Tianjin 300072, People's Republic of China

<sup>2</sup>School of Electrical and Computer Engineering, Oklahoma State University, Stillwater, Oklahoma 74078, USA

<sup>3</sup>Center for Integrated Nanotechnologies, Materials Physics and Applications Division, Los Alamos National Laboratory, Los Alamos, New Mexico 87545, USA

<sup>4</sup>School of Physics and Astronomy, University of Birmingham, Birmingham B15 2TT, United Kingdom

(Received 9 January 2011; accepted 7 March 2011; published online 24 March 2011)

We investigate resonant transmission of planar asymmetric metamaterials made from double split-ring resonators. As the symmetry of the unit cell resonator is broken by displacing the two gaps away from the center in opposite directions, a giant amplitude modulation is observed at the fundamental inductive-capacitive resonance due to strong polarization conversion. The modulation is nearly absent when the gaps are moved together in the same direction. This effect persists in metamaterials with different structural designs. These asymmetric metamaterials may open up new avenues toward the control of terahertz waves and the development of modulator and polarizer based terahertz devices. © 2011 American Institute of Physics. [doi:10.1063/1.3571288]

Metamaterials, with artificial electromagnetic response not attainable with naturally occurring materials, have shown numerous intriguing effects, such as negative refraction,<sup>1–4</sup> cloaking,<sup>5</sup> and superfocusing.<sup>6</sup> During the past decade, multiple structures have been proposed for the landmark predictions of metamaterial theory, including split-ring resonators (SRRs),<sup>7,8</sup> fishnets,<sup>2,4,9</sup> and other stereostructures.<sup>10,11</sup> Planar metamaterials, with its ease of fabrication, are made from thin metal films with periodic structures at subwavelength scale unit size. Through asymmetric design, the tiny structural refinement may dramatically modify the electromagnetic wave propagation.<sup>12–16</sup> Terahertz technologies hold the promise for broad applications such as security detection<sup>17</sup> and molecule sensing,<sup>18</sup> however, the shortage for devices that can effectively manipulate terahertz waves is constraining their further development. Metamaterials, for its design flexibility, have potential in developing unique integrated devices and components to fill the “Terahertz Gap.”<sup>19–24</sup> Simultaneous control of the metamaterial resonances and the incident terahertz wave polarization may provide additional degrees of freedom.

In this letter, we investigate the response of metamaterials to terahertz radiation by gradually displacing the two gaps of the double SRRs in opposite directions from the center, thus breaking the mirror symmetry of the structure (Fig. 1). Through experiments and numerical simulations, we find that symmetry breaking induces a strong amplitude modulation at the inductive-capacitive (LC) resonance. The modulation is originated from the polarization conversion of the incident terahertz wave from linear to elliptical due to asymmetric electric field distribution in the SRRs.

The planar metamaterial samples are characterized by broadband (0.1–4.5 THz) terahertz time-domain spectroscopy (THz-TDS).<sup>24,25</sup> An 8-*f* confocal THz-TDS system fo-

cuses the beam to a 3.5 mm diameter waist which enables a frequency-independent condition for small sample characterization. Five sets of planar SRR metamaterials with 200-nm-thick Al structures are fabricated on a 640- $\mu\text{m}$ -thick p-type silicon substrate by use of optical lithography. Figure 1(a) shows the general schematic of THz-TDS measurement with a size of the sample array 1.5 cm  $\times$  1.5 cm. The diagram of

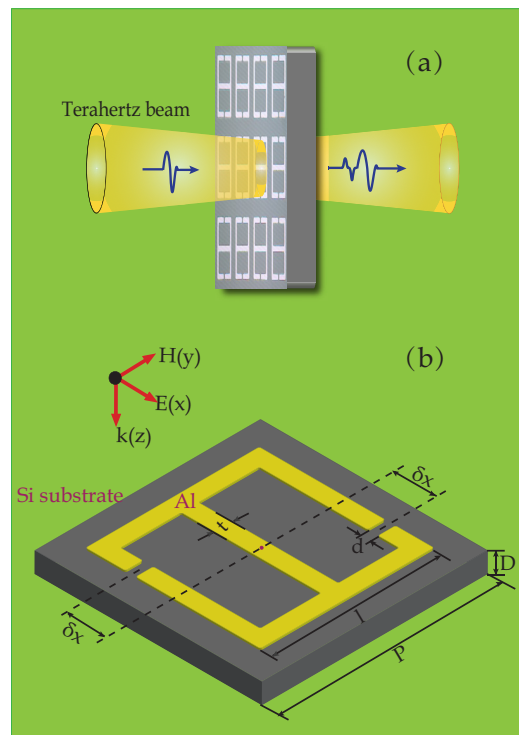


FIG. 1. (Color online) (a) Experimental configuration for the terahertz transmission measurements of a periodic array of planar metamaterials. (b) Schematic of the rectangular double SRR unit cell and the silicon substrate with a minimum feature  $d=3\ \mu\text{m}$  in the splits of the rings and other structural dimensions  $t=5\ \mu\text{m}$ ,  $l=50\ \mu\text{m}$ , and a lattice periodicity  $P=65\ \mu\text{m}$ .

<sup>a)</sup>Electronic mail: jiaghan@tju.edu.cn.

<sup>b)</sup>Electronic mail: weili.zhang@okstate.edu.

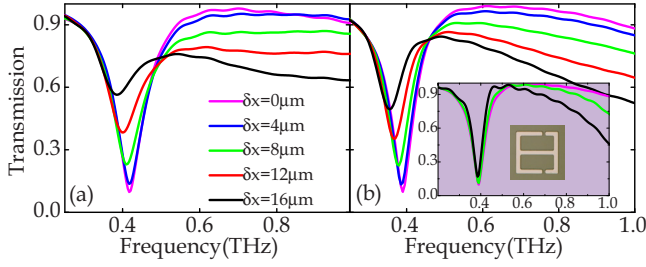


FIG. 2. (Color online) Measured (a) and simulated (b) amplitude transmission spectra of the rectangular double SRRs with varying asymmetry. The inset of (b) shows transmission spectra of the equidirectionally displaced rectangular SRRs with  $\delta x=0, 8, 16 \mu\text{m}$ , respectively.

a rectangular SRR unit cell is shown in Fig. 1(b). Asymmetry in the SRRs is introduced by displacing the gaps gradually away from the center by  $\delta x=0, 4, 8, 12, 16 \mu\text{m}$ , respectively.

A sharp LC resonance is excited if the incident electric field is oriented along the  $x$  axis, i.e., perpendicular to the two gaps in each SRR. The amplitude transmission is obtained by  $|\tilde{t}(\omega)|=|\vec{E}_{Sx}(\omega)/\vec{E}_{Rx}(\omega)|$ , where  $\vec{E}_{Sx}(\omega)$  and  $\vec{E}_{Rx}(\omega)$  are Fourier transformed transmitted electric field of the signal and reference pulses, respectively. Figure 2(a) shows the measured transmission spectra  $|\tilde{t}(\omega)|$  through the samples with different levels of asymmetry. For the symmetric structure with centered gaps, the transmission shows a resonance dip approaching 10% at 0.42 THz with a quality factor (Q) around 7.6. When asymmetry is introduced by displacing the two gaps in the SRR,  $|\tilde{t}(\omega)|$  increases significantly to 60% at  $\delta x=16 \mu\text{m}$  while the resonance frequency redshifts from 0.42 to 0.38 THz with the Q factor decreasing to 3.9. Interestingly, for the SRR patterns with two gaps displaced along the same direction, as shown in the inset of Fig. 2(b), the transmission spectra exhibit much less modulation and frequency shift with varying  $\delta x$ , indicating that the large amplitude modulation and frequency shift for the asymmetric patterns presented in Fig. 2(a) are associated with the lack of mirror symmetry in each unit resonator.

To elucidate the mechanism underlying the observed spectra characteristics of the asymmetric SRRs, finite-element numerical simulations were carried out using CST Microwave Studio. The unit cell shown in Fig. 1(b) was used in the simulations with a periodic boundary condition. The silicon substrate was modeled as a lossless dielectric  $\epsilon=11.78$  and Al had a conductivity of  $\sigma=3.72 \times 10^7 \text{ S m}^{-1}$ . The simulated transmissions  $|\tilde{t}(\omega)|$  of the SRRs for different  $\delta x$ , as shown in Fig. 2(b) match well with all the experimental results given in Fig. 2(a). The weakening of the resonance with increasing asymmetry is due to the reduced coupling of the metamaterial structure with the free space.<sup>14</sup> The minor redshift is due to increased parasitic capacitance between the nearest neighbor SRRs as the gaps are moved away from the center leading to a redistribution of charges in the rings and an increase in the effective capacitance.

We analyze the electric field and current distributions of the SRRs, and find that the polarization of the incident wave is dramatically changed for all the asymmetric SRRs. As shown in the simulated far-field electrical field distribution in Fig. 3(a), the polarization of the incident wave was converted from linear into elliptical for  $\delta x \neq 0$  at the LC resonance. With increasing asymmetry, the azimuth and ellipticity of the ellipse change monotonically. Figures 3(d) and 3(e) depict

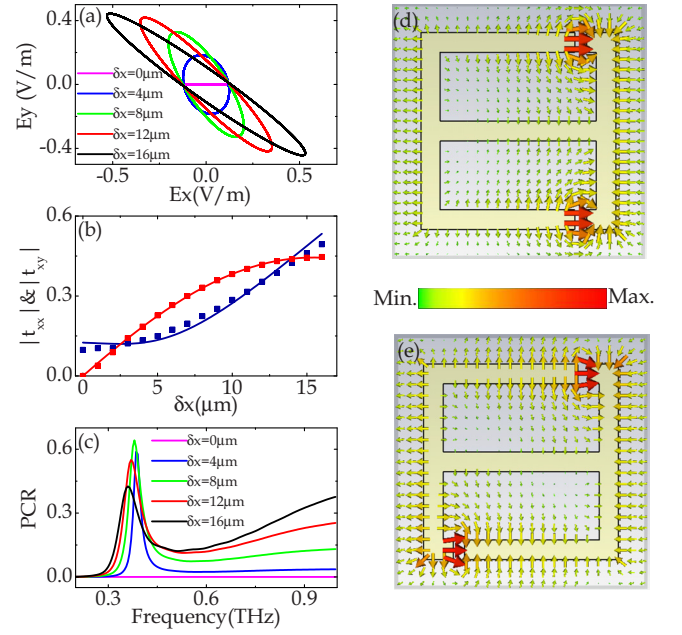


FIG. 3. (Color online) (a) Simulated far-field electric field distribution of the rectangular SRRs with varying asymmetry at the LC resonance. (b) The upper and lower squares represent the numerical dip values of  $|\tilde{t}_{xy}|$  and  $|\tilde{t}_{xx}|$  at resonance frequency, respectively. The blue and red lines represent the fitting curves, in which  $\alpha=0.513$ ,  $b=-0.009$ ,  $c=0.095$ , and  $\varphi=2.9$ . (c) PCR with varying asymmetry. [(d) and (e)] Simulated surface electric field distribution of equidirectionally (d) and oppositely (e) displaced SRRs with  $\delta x=16 \mu\text{m}$ .

the electric field distributions at the LC resonance with the gaps displaced  $16 \mu\text{m}$  away from the center but along the same and opposite directions, respectively. The arrows indicate instantaneous directions of the electric field. In both cases, the electric field distribution at the corners close to the gaps indicates excitation of dipole moment along the  $y$  direction. As expected, for the equidirectional case, the electric field shows mirror symmetric distributions [Fig. 3(d)]. The far-field  $\vec{E}$  vector only has the component along  $x$  axis, while along  $y$  axis, it equals zero due to the cancellation of contribution from the two gaps of each SRR. On the contrary, when the gaps are oppositely displaced from the center of the SRRs, i.e., mirror symmetry is broken, the contribution from the gaps adds up constructively along the  $y$  axis at far field, therefore inducing strong transmission modulations and polarization conversion at the LC resonance.

The main features of the aforementioned mechanism can be understood with the help of simple electromagnetic wave equations. To achieve the transmission consistent with the experimental measurements around resonance frequency  $\omega_0$ , we consider the  $\vec{E}$  vector through the reference (blank Si) as follows:

$$\vec{E}_{Rx}(\omega) = E_0 e^{i(kz - \omega t)} \hat{e}_x. \quad (1)$$

The incident linear wave interacts with the SRRs and thus has  $x$  and  $y$  components as follows:

$$\vec{E}_{Sx}(\omega) = E_0 [(1 - ae^{b\delta x}) + ae^{b\delta x} \cos(c\delta x) e^{-i\varphi}] e^{i(kz - \omega t)} \hat{e}_x, \quad (2)$$

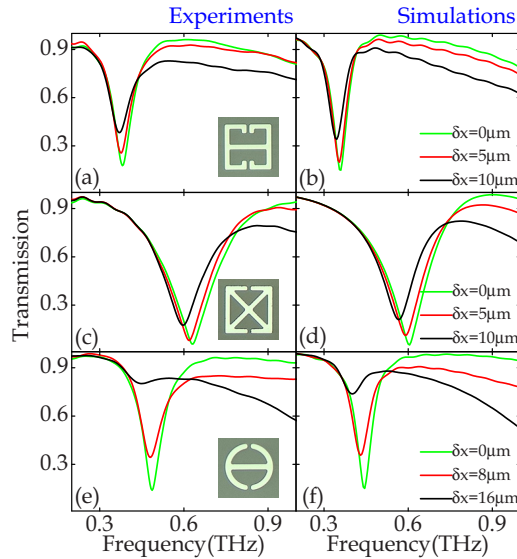


FIG. 4. (Color online) Measured (a) and simulated (b) amplitude transmission spectra of the capacitor-enhanced double SRRs with varying asymmetry. [(c) and (d)] show the measured and simulated spectra of the crossed double SRRs. [(e) and (f)] show the measured and simulated spectra of the circular double SRRs.

$$\vec{E}_{S_y}(\omega) = E_0 \alpha e^{b\delta x} \sin(c\delta x) e^{i(kz - \omega t - \varphi)} \hat{e}_y, \quad (3)$$

where  $\alpha e^{b\delta x}$  is the coupling coefficient between the incident field and the SRRs, and  $\cos(c\delta x)$  and  $\sin(c\delta x)$  represent the parallel and perpendicularly coupled-out coefficient, respectively. We thus have the amplitude transmissions:  $|\tilde{t}_{xx}(\omega)| = |\vec{E}_{S_x}(\omega)/\vec{E}_{Rx}(\omega)|$  and  $|\tilde{t}_{xy}(\omega)| = |\vec{E}_{S_y}(\omega)/\vec{E}_{Rx}(\omega)|$ . The solid squares in Fig. 3(b) show the simulated dip values of  $|\tilde{t}_{xx}(\omega)|$  and  $|\tilde{t}_{xy}(\omega)|$  at the resonance frequency for different  $\delta x$ . The solid lines are fittings based on the above  $\vec{E}$ -vector equations. The fitting curve reproduces the numerical data quite well, which corroborates our model for quantitative understanding the results from numerical simulations. According to Ref. 26, we introduce a polarization conversion rate (PCR) as  $\text{PCR} = |\tilde{t}_{xy}(\omega)|^2 / (|\tilde{t}_{xx}(\omega)|^2 + |\tilde{t}_{xy}(\omega)|^2)$ . Figure 3(c) shows the calculated PCR for different samples, where we found the maximum polarization conversion is observed for the sample with  $\delta x = 8 \mu\text{m}$  and its PCR is more than 60% around the resonance frequency.

To further optimize amplitude modulation of the LC resonance in the planar asymmetric metamaterial patterns, we also design and fabricate other SRR samples with different configurations. We use a capacitance-enhanced structure, by adding up the dimension of the capacitors at the gaps, to attenuate the long side arm coupling effect. The measured and simulated transmission amplitudes of which, as shown in Figs. 4(a) and 4(b), respectively with  $\delta x = 0, 5, 10 \mu\text{m}$ , indicate a much less profound frequency shift and Q factor modulation. A crossed structure, as shown in Figs. 4(c) and 4(d) also displays a clear amplitude modulation at the LC resonance but less significant because of their lower level of asymmetry due to original design limitations in the structure. Figures 4(e) and 4(f) show the measured and simulated transmission spectra of circularly configured SRRs with varying asymmetry, in which an even stronger LC resonance amplitude modulation of 66%, compared to the rectangular configuration of 50%, is observed. This could be explained by a

distinct variation in the capacitance value due to changes in the opposite areas of the gaps.

In summary, we show that introducing asymmetry in the double SRR metamaterials enables the control of wave transmission and polarization conversion at terahertz frequencies. The fundamental LC resonance amplitude can be strongly modulated along with a minor shift in resonance frequency. The polarization of the incident wave after transmitting through the metamaterial can also be controlled due to asymmetry in the structure. This substantial modulation and polarization conversion effect may provide an alternative toward manufacturing terahertz modulators and polarizers in which the SRR structure could be reconfigured,<sup>27</sup> thus providing a gateway for integrated device applications, such as frequency selection, biosensing, and polarizing in the terahertz regime.

This work was supported by the U.S. National Science Foundation (Grant No. ECCS-0725764), the National Science Foundation of China (Grant Nos. 61028011, 61007034, and 60977064), the Tianjin Sci-Tech Program (Grant Nos. 09ZCKFGX01500 and 10JCYBJC01400), and the MOE 111 Program of China (Grant No. B07014).

- <sup>1</sup>R. A. Shelby, D. R. Smith, and S. Schultz, *Science* **292**, 77 (2001).
- <sup>2</sup>J. Valentine, S. Zhang, T. Zentgraf, E. Ulin-Avila, D. A. Genov, G. Bartal, and X. Zhang, *Nature (London)* **455**, 376 (2008).
- <sup>3</sup>S. Zhang, Y. Park, J. Li, X. Lu, W. Zhang, and X. Zhang, *Phys. Rev. Lett.* **102**, 023901 (2009).
- <sup>4</sup>J. Gu, J. Han, X. Lu, R. Singh, Z. Tian, Q. Xing, and W. Zhang, *Opt. Express* **17**, 20307 (2009).
- <sup>5</sup>J. Valentine, J. Li, T. Zentgraf, G. Bartal, and X. Zhang, *Nature Mater.* **8**, 568 (2009).
- <sup>6</sup>J. B. Pendry, *Phys. Rev. Lett.* **85**, 3966 (2000).
- <sup>7</sup>J. B. Pendry, A. J. Holden, D. J. Robbins, and W. J. Stewart, *IEEE Trans. Microwave Theory Tech.* **47**, 2075 (1999).
- <sup>8</sup>R. Marqués, J. Martel, F. Mesa, and F. Medina, *Phys. Rev. Lett.* **89**, 183901 (2002).
- <sup>9</sup>S. Zhang, W. Fan, N. C. Panoiu, K. J. Malloy, R. M. Osgood, and S. R. Brueck, *Opt. Express* **14**, 6778 (2006).
- <sup>10</sup>E. Plum, J. Zhou, J. Dong, V. A. Fedotov, T. Koschny, C. M. Soukoulis, and N. I. Zheludev, *Phys. Rev. B* **79**, 035407 (2009).
- <sup>11</sup>N. Liu, H. Liu, S. Zhu, and H. Giessen, *Nat. Photonics* **3**, 157 (2009).
- <sup>12</sup>V. A. Fedotov, M. Rose, S. L. Prosvirnin, N. Papasimakis, and N. I. Zheludev, *Phys. Rev. Lett.* **99**, 147401 (2007).
- <sup>13</sup>I. Al-Naib, C. Jansen, and M. Koch, *Appl. Phys. Lett.* **94**, 153505 (2009).
- <sup>14</sup>R. Singh, I. Al-Naib, M. Koch, and W. Zhang, *Opt. Express* **18**, 13044 (2010).
- <sup>15</sup>R. Singh, E. Plum, W. Zhang, and N. I. Zheludev, *Opt. Express* **18**, 13425 (2010).
- <sup>16</sup>R. Singh, I. A. I. Al-Naib, M. Koch, and W. Zhang, *Opt. Express* **19**, 6312 (2011).
- <sup>17</sup>Y. C. Shen, T. Lo, P. F. Taday, B. E. Cole, W. R. Tribe, and M. C. Kemp, *Appl. Phys. Lett.* **86**, 241116 (2005).
- <sup>18</sup>M. Nagel, P. Haring Bolivar, M. Brucherseifer, H. Kurz, A. Bosserhoff, and R. Buttner, *Appl. Phys. Lett.* **80**, 154 (2002).
- <sup>19</sup>H. Chen, W. J. Padilla, J. M. O. Zide, A. C. Gossard, A. J. Taylor, and R. D. Averitt, *Nature (London)* **444**, 597 (2006).
- <sup>20</sup>T. J. Yen, W. J. Padilla, N. Fang, D. C. Vier, D. R. Smith, J. B. Pendry, D. N. Basov, and X. Zhang, *Science* **303**, 1494 (2004).
- <sup>21</sup>J. Han, A. Lakhtakia, and C.-W. Qiu, *Opt. Express* **16**, 14390 (2008).
- <sup>22</sup>R. Singh, Z. Tian, J. Han, C. Rockstuhl, J. Gu, and W. Zhang, *Appl. Phys. Lett.* **96**, 071114 (2010).
- <sup>23</sup>J. Gu, R. Singh, Z. Tian, W. Cao, Q. Xing, M. He, J. W. Zhang, J. Han, H. Chen, and W. Zhang, *Appl. Phys. Lett.* **97**, 071102 (2010).
- <sup>24</sup>A. K. Azad, J. Dai, and W. Zhang, *Opt. Lett.* **31**, 634 (2006).
- <sup>25</sup>D. Grischkowsky, S. Keiding, M. van Exter, and C. Fittinger, *J. Opt. Soc. Am. B* **7**, 2006 (1990).
- <sup>26</sup>J. Hao, Y. Yuan, L. Ran, T. Jiang, J. A. Kong, C. T. Chan, and L. Zhou, *Phys. Rev. Lett.* **99**, 063908 (2007).
- <sup>27</sup>H. Tao, A. C. Strikwerda, K. Fan, W. J. Padilla, X. Zhang, and R. D. Averitt, *Phys. Rev. Lett.* **103**, 147401 (2009).